RESEARCH

Efficient passively *Q*-switched Nd: KGW/Cr^{4+}:YAG self-Raman laser

Qiaoshuang Zou[1] · Qinghu Sun[1] · Zhenhong Dai[1] · Shuanghong Ding[1]

Abstract

In this paper, the end-pumped passively *Q*-switched Nd: KGW/Cr^{4+}:YAG self-Raman laser is designed to achieve high efficient operation. Concave-plane linear cavity is adopted to obtain the shortest cavity length, and long Nd: KGW crystal of 40 mm is used in the experiment. Cr^{4+}:YAG crystals of high initial transmittances ($T_0 = 96\%$ and 92%) are utilized to realize efficient and stable passively *Q*-switched operation. The passively *Q*-switched Nd: KGW/Cr^{4+}:YAG self-Raman laser is theoretically investigated at 1181 nm corresponding to the Raman mode of 901 cm^{-1} shift in Nd: KGW crystal. With Cr^{4+}:YAG crystal of the initial transmittance $T_0 = 96\%$, the maximum output power of 0.624 W at 1181 nm is achieved experimentally with optical-to-optical efficiency of 13.9%, which is the highest efficiency reported for passively *Q*-switched Nd: KGW self-Raman laser.

1 Introduction

Nd: KGd(WO$_4$)$_2$ (Nd: KGW) crystal is a good laser medium, and possesses long fluorescence lifetime, high optical quality and high laser efficiency [1]. KGW crystal also stands out as an efficient Raman medium, boasting large Raman gain, excellent thermal conductivity, and a high damage threshold. The monoclinic structure of KGW crystals imparts anisotropic optical properties, and offers a unique advantage with two strong Raman lines at 768 cm^{-1} and 901 cm^{-1} orthogonally polarized, each exhibiting similar Raman gains.

KGW crystal based Raman laser have been researched with different configurations, such as Raman generator [2–4], CW intracavity Raman laser [5–10], actively or passively *Q* switched intracavity Raman laser [11–17], self-Raman laser [18–21], etc.

In 2005, H. M. Pask reported the continuous-wave (CW) operation of a diode-pumped Nd: YAG/KGW solid-state Raman laser, achieving an output power of 800 mW at first Stokes 1176 nm with a conversion efficiency of 4% [5]. In 2020, Y. F. Chen et al. developed an efficient diode-pumped CW Nd: YVO$_4$/N_p-cut KGW Raman yellow laser.

First Stokes at 1159 nm was generated by SRS process of Raman mode at 768 cm^{-1}, and yellow laser at 579.5 nm was obtain by second harmonic generation. At a pumping power of 30 W, the yellow laser output power at 579.5 nm reached 6.8 W [8]. In 2023, J. N. Geng et al. investigated CW Nd: YVO$_4$/KGW Raman laser. With a laser diode pumping power of 36.65 W, the output power of first Stokes laser at 1177 nm reached 9.33 W [9].

Incorporating a *Q*-switching device into the laser resonator enables the generation of pulsed laser output. In 2020, S. B. Dai et al. realized an actively *Q*-switched eye-safe Nd: YLF/KGW intracavity Raman laser. Under conditions of a pumping power of 46.9 W and an optimal repetition frequency of 4 kHz, they obtained a maximum average output power of 3.6 W at 1461 nm [12]. More recently, H. Zhao et al. adopted the acousto-optically *Q*-switched Nd: YLF/KGW Raman laser to achieve a multi-wavelength deep red laser output [13, 14]. Utilizing the Raman modes of 768 cm^{-1} and 901 cm^{-1}, first Stokes laser at 1461 nm and 1490 nm were generated, which were subsequently converted with LBO crystals into deep red emission lines at 731 nm and 745 nm, respectively. With a pumping power of 83 W, the maximum average output power at 731 nm and 745 nm are of 5.2 W and 7.6 W, respectively [14].

Passively *Q*-switching is renowned for its simplicity, compactness, and lower costs. In 2010, H. W. Yang et al. utilized an Nd: YAG/Cr: YAG/Nd: KGW laser to generate first Stokes laser at 1181 nm. With a laser diode pumping power of 5.74 W, they achieved an average output power

✉ Shuanghong Ding
  shding@ytu.edu.cn

[1] School of Physics and Electronic Information, Yantai University, Yantai 264005, P.R. China

of 336 mW at the first Stokes wavelength [15]. In 2023, J. C. Chen et al. proposed a compact passively Q-switched Nd: YVO$_4$/KGW/Cr: YAG yellow Raman laser [16, 17]. By selectively directing the polarization direction of the fundamental laser along the N_g or N_m axis of the KGW crystal, yellow laser at 579 nm or orange laser at 589 nm could be generated. The optimal optical-to-optical conversion efficiencies for the yellow and orange lasers were 11.5% and 11.0%, respectively [17].

Self-Raman laser can reduce the number of optical components inside the laser cavity, making the laser structure more compact. This not only reduces intracavity losses but also lowers the laser's threshold. In 2000, A. S. Grabtchikov introduced a passively Q-switched laser diode pumped Nd: KGW/Cr: YAG Raman laser. With the fundamental laser at 1.067 μm, first Stokes at 1.181 μm and first anti-Stokes laser at 0.973 μm were generated. For the pumping power of 230 mW, a maximum output power of 4.8 mW for the first Stokes laser was realized [18]. In 2007, V. A. Lisinetskii et al. achieved CW Nd: KGW/KGW self-Raman laser. At a pumping power of 2 W, they obtained the first Stokes output power of 277 mW [19]. In 2010, A. J. Lee reported on a CW Nd: KGW intracavity frequency-doubled self-Raman laser, generating 450 mW at 590 nm [20]. In 2015, Y. Tang et al. achieved a high efficient CW Nd: KGW self-Raman laser using a Raman mode of 89 cm^{-1}. At a pumping power of 2.5 W, the maximum output power of first Stokes laser reached 0.42 W [21].

Due to the advantages of passively Q switching and self-Raman configuration, Nd: KGW/Cr: YAG self-Raman laser can realize compact pulsed laser. However, the reported performance of Nd: KGW/Cr: YAG self-Raman laser was far from optimization [18]. In this paper, the laser is designed and optimized. The performance of Nd: KGW/Cr: YAG self-Raman laser at 1181 nm is promoted greatly. With a pumping power of 4.5 W, we attained a maximum output power of 0.624 W at 1181 nm, with an optical-to-optical efficiency of 13.8%. The single-pulse energy reached 14.1 μJ, while the peak power is calculated to be 0.59 MW. These results represent the highest conversion efficiency reported up to date for passively Q-switched Nd: KGW self-Raman lasers.

2 Resonator design

Rate equations are powerful tools for analyzing performances of Q-switched lasers. Transverse distributions of laser beams significantly influent the intracavity nonlinear processes, such as stimulated Raman scattering and saturable absorption. Space-dependent rate equations of passively Q-switched intracavity Raman lasers were deduced by our

group [22]. It was found the Raman gain and the saturable absorber factor is closely related to the resonator structure.

For efficient operation of passively Q-switched Nd: KGW/Cr^{4+}:YAG self-Raman laser, the saturable absorber parameter α and normalized Raman gain M are two decisive parameters. α is a synthetic parameter representing how easily the saturable absorber is bleached, and is defined as [22]

$$\alpha = k_{la}^2 \frac{\gamma_A \sigma_{gsa}}{\gamma_L \sigma} \tag{1}$$

,where σ_{gsa} is the ground-state absorption cross section of the saturable absorber, σ the stimulated emission cross-section of the laser medium, γ_L and γ_A the inversion reduction factors of laser and saturable absorber media, respectively. k_{la} is the ratio of the fundamental laser beam size in the laser medium to that in the saturable absorber.

With greater α, fundamental laser pulses of narrower pulse width and higher peak intensity will be generated, and more efficient SRS conversion inside the resonator will be achieved. As shown in (1), α is inversely proportional to the stimulated emission cross-section of the laser medium σ. For Nd: KGW crystal, σ is 1.48×10^{-18} cm^{-2}. As comparison, σ is 1.8×10^{-19} cm^{-2} and 2.8×10^{-19} cm^{-2} for Nd: YLF and Nd: YAG crystals, respectively. Due to the much higher σ, the good performance of passively Q-switched Nd: KGW laser is more difficult. However, besides the features of the laser and saturable absorb media, α is also related to k_{la} as depicted in (1). Therefore, large α can be obtained through the appropriate resonator design.

The normalized Raman gain M is defined as [22]

$$M = \frac{k_{ls}^2}{2} \frac{g h v_S c l_S}{\gamma_L \sigma l_c} \tag{2}$$

,where g is the Raman gain coefficient of the Raman medium, h the Plank constant, c is the light speed in the vacuum, v_S the frequency of first Stokes beam, l_S the length of Raman medium, and l_c the cavity optical length. k_{ls} is to the ratio of the fundamental laser beam size in the laser medium to that in the Raman medium.

Great M is appreciated for efficient Raman laser. M is related to the characteristics of Raman medium as shown in (2), e.g. g and l_S, and also related to characteristics of the laser medium, i.e. the stimulated emission cross-section σ. Unfortunately, having great σ, Nd: KGW crystal yields small M, which results in high SRS threshold. However, as shown in (2), short cavity length l_c and long Nd: KGW crystal length can result in great M. In fact, for a given Raman crystal, there is a minimum limit on the length of the resonant cavity. In the experiment, for the Raman crystal of the
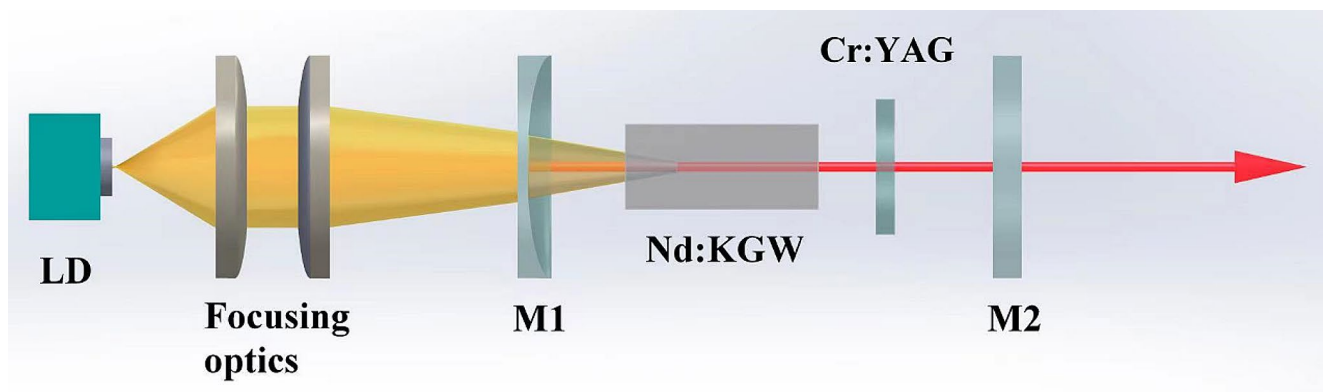
Fig. 1 Setup of passively *Q*-switched Nd: KGW self-Raman laser
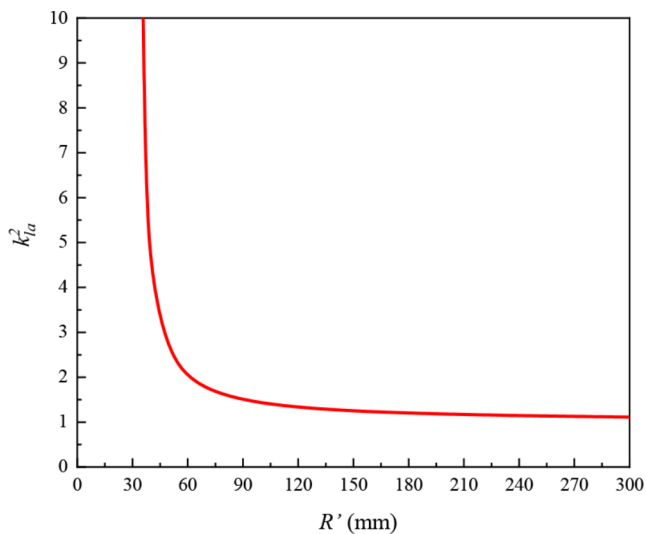
Fig. 2 Squared beam size ratio k^2_{la} versus equivalent curvature radius *R*'

given length, the cavity length can be compressed as far as possible to improve M.

For passively *Q*-switched laser, features of laser pulses are closely related to the initial transmission of Cr⁴⁺:YAG T_0. Again due to much great σ of Nd: KGW crystal, more efficient and stable operation of passively *Q*-switched Nd: KGW can be obtained for greater T_0, and laser operation deteriorates as T_0 decreasing. However, smaller T_0 leads to fundamental laser pulses of smaller pulse energy, larger pulse width and smaller pulse peak intensity, and greater α and M is required to achieve efficient passively *Q*-switched Nd: KGW self-Raman laser.

Based on the above analysis, the passively *Q*-switched Nd: KGW/Cr⁴⁺:YAG self-Raman laser is designed as shown in Fig. 1 to achieve high efficient operation. To obtain great M, the two-mirror linear cavity is adopted to obtain the shortest cavity length, which is 55 mm, and long Nd: KGW crystal of 40 mm is used in the experiment. The input mirror M1 is a concave mirror with curvature radius R_1, and

plane output mirrors are adopted. In the resonator, the beam waist is located on the output mirror, to which Cr⁴⁺:YAG crystals are placed adjacently. For LD end pumped laser, the focal length *f* of laser medium thermal lens decreases as pumping power increases. Taking thermal lens and con-caved input mirror into consideration, the equivalent curva-ture radius *R*' is $2f R_1/(2f + R_1)$, and decreases as pumping power increases. Squared beam size ratio k^2_{la} varies with the equivalent curvature radius *R*' as shown in Fig. 2. In this paper, the curvature radius R_1 of input mirror is chosen to be 150 mm, and k^2_{la} is greater than 1.25 to obtain great α. Cr⁴⁺:YAG crystals of high initial transmittances ($T_0 = 96\%$ and 92%) are utilized to realize efficient and stable passively *Q*-switched operation.

## 3 Experimental investigations on fundamental laser

3.1 Experimental setup

The setup of passively *Q*-switched Nd: KGW laser is depicted in Fig. 1. A fiber-coupled semiconductor laser serves as the pumping source at a central wavelength of 808 nm. The fiber diameter is 400 μm with a numerical aperture of 0.22. Following the pumping source is a cou-pling mirror, having a coupling efficiency of 95%. The input mirror M1, is a concave mirror with a curvature radius of 150 mm, coated with a high-transmission film ($T = 96.7\%$) for the pumping laser and a high-reflectance film for wave-lengths between 1000 and 1200 nm.

The N_p-cut Nd: KGW crystal is employed with dimen-sions of $3 \times 3 \times 40$ mm³ and a doping concentration of 3%. It is equipped with anti-reflective coatings for wavelengths of 808 nm, 1067 nm and 1181 nm ($R < 0.2\%$@1067 nm, $R < 0.5\%$@1181 nm, and $R < 3\%$@808 nm). Two Cr⁴⁺:YAG crystals with different initial transmittances (T_0) are utilized, which are 96% and 92%, respectively. The total cavity
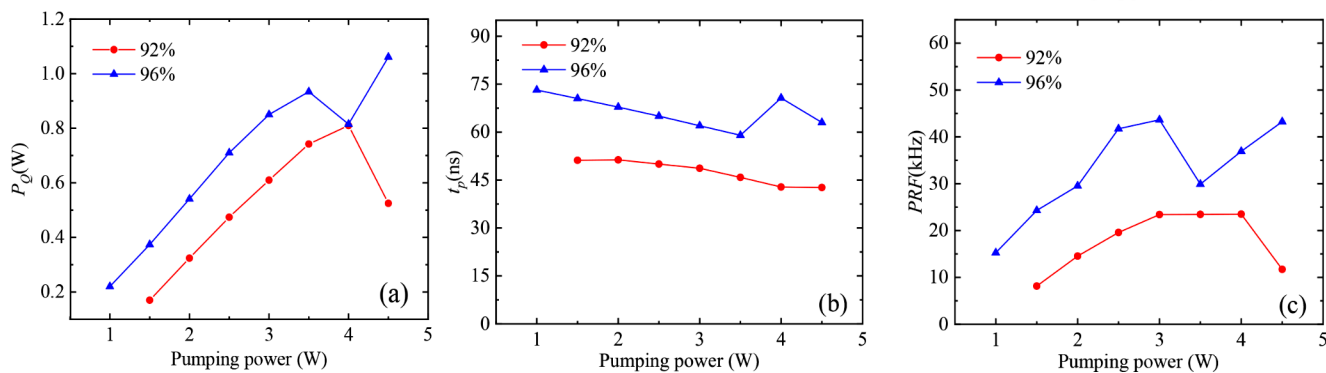
Fig. 3 The output characteristics of the fundamental laser include (**a**) output power, (**b**) pulse width, and (**c**) PRF, where the circular and triangle symbols correspond to Cr^{4+}:YAG with initial transmittances of 92% and 96%, respectively

Fig. 4 For the pumping power of 3 W, pulse sequences and pulse waveforms of the fundamental laser are given. (**a**) and (**b**) are for Cr^{4+}:YAG of initial transmittance $T_0 = 92\%$, (**c**) and (**d**) are for $T_0 = 96\%$
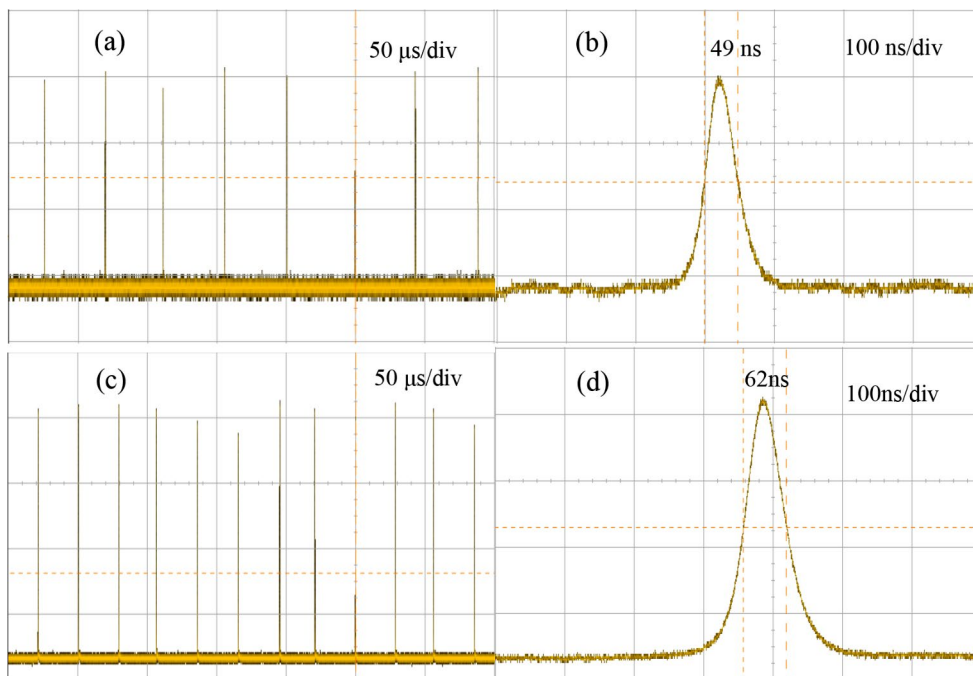
length is 5 cm. Furthermore, all crystals are water-cooled to maintain a constant temperature of 24 °C.

During the experiment, the average laser output power is monitored by using a power meter (Ophir Laserstar). To visualize the temporal characteristics of the laser output, a digital oscilloscope (Agilent, DSO7104A) equipped with a fast PIN photodiode is employed. The output laser spectrum is analyzed by a spectrometer (Zolix Omni-λ3008).

3.2 Output characteristics of fundamental laser output

In the preliminary phase, the output characteristics of the fundamental laser are investigated using the experimental configuration illustrated in Fig. 1. The output mirror, M2, is the flat mirror with 90% reflectance at 1067 nm. These

output characteristics are illustrated in Fig. 3, where circular and triangle symbols represent Cr^{4+}:YAG initial transmittances of 92% and 96%, respectively. The output power, pulse width, and pulse repetition frequency (PRF) are depicted in Fig. 3(a), (b) and (c), respectively.

As illustrated in Fig. 3(a), with the same Cr^{4+}:YAG crystal, the output power of the fundamental laser increases proportionally with the pumping power. For a pumping power of 4.5 W and a Cr^{4+}:YAG of initial transmittance 96%, the maximum output power reaches 1.06 W, achieving an optical-to-optical efficiency of 23.5% and a pulse energy of 24.5 μJ.

Figure 3(b) illustrates that the pulse width of the fundamental laser elongates with Cr^{4+}:YAG of higher initial transmittance. The shortest pulse width of the fundamental laser of 42.7 ns is observed when the Cr^{4+}:YAG initial

Table 1 Parameters of the output mirror M2

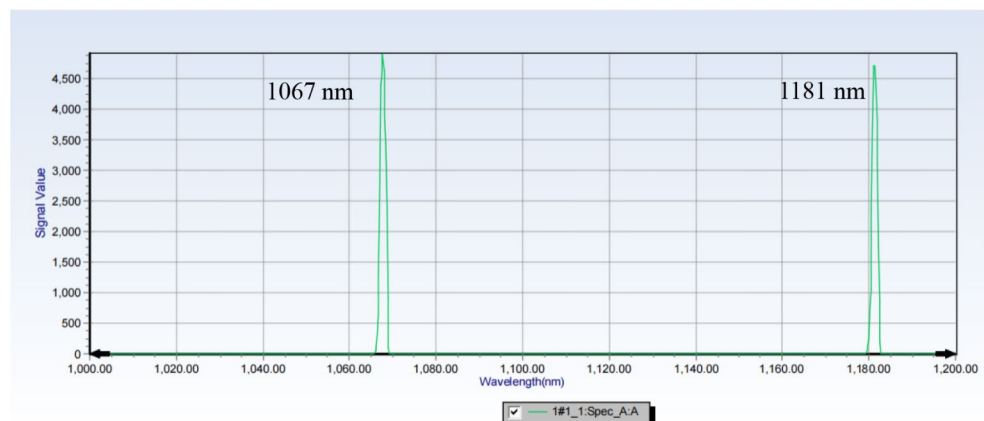| Output mirror	Coating specifications
S1(#30)	$R = 99.9\%@1067$ nm, $R = 88.40\%@1181$ nm
S2(#31)	$R = 99.9\%@1067$ nm, $R = 82.9\%@1181$ nm
S3(#32)	$R = 99.9\%@1067$ nm, $R = 70.2\%@1181$ nm
S4(#33)	$R = 99.9\%@1067$ nm, $R = 83.8\%@1181$ nm

transmittance is 92%. In Fig. 3(c), PRF of the fundamental laser elevates with Cr^{4+}:YAG of higher initial transmittance. For a pumping power of 4.5 W and Cr^{4+}:YAG of initial transmittance 96%, the maximum PRF registers at 43.2 kHz.

For Cr^{4+}:YAG of initial transmittances 92%, the output power drops at a pumping power of 4.5 W due to cavity instability induced by the thermal lens effect of the laser crystal. For the Cr^{4+}:YAG with initial transmittance of 96% and the pumping power of 4 W, a decline in output power is also observed due to the thermal lens effect. The Cr^{4+}:YAG crystal with a higher initial transmittance mitigates the thermal lens effect of the laser crystal, although it exacerbates the thermal effect of the Cr^{4+}:YAG crystal with initial transmittance of 96% itself. Consequently, at a pumping power of 4.5 W, the thermal lens effect of the Cr^{4+}:YAG crystal with initial transmittance of 96% partially counteracts the thermal lens effect of the laser crystal on cavity stability, thus in output power of the fundamental laser restores the increasing trend.

The temporal characteristics of the fundamental laser are presented in Fig. 4. At a pumping power of 3 W, for Cr^{4+}:YAG of initial transmittance $T_0 = 92\%$, the pulse sequence and waveform of fundamental laser are given in (a) and (b). Similarly, for $T_0 = 96\%$, those are given in (c) and (d).

As shown in Fig. 4 (a) and (c), pulse sequences exhibit high stability, and with increasing initial transmittance of the saturable absorber, the pulse sequences become more densely packed. As shown in In Fig. 4 (b) and (d), as the initial transmittance of the saturable absorber increases, the pulse width of the pulse waveform expands.

Due to large emission cross section of Nd: KGW, good performance of passively *Q*-switched laser is not realized with the saturable absorber of low initial transmittance (89%).

# 4 Experimental investigations on first Stokes laser output

4.1 Experimental setup

The experimental setup for the passively *Q*-switched Nd: KGW/Cr⁴⁺:YAG self-Raman laser is depicted in Fig. 1. The output mirror (M2) is a flat mirror, and four output mirrors of different specifications (S1, S2, S3 and S4) are utilized in the experiments as given in Table 1. Two Cr^{4+}:YAG crystals with initial transmittances of 96% and 92% are employed in the experiments, which are positioned between the Nd: KGW crystal and the output mirror. The total cavity length is 5.5 cm. All crystals are water-cooled, maintaining a temperature of 24 °C.

4.2 Output characteristics of first Stokes laser at 1181 nm

Experiments are conducted on a passively *Q*-switched Nd: KGW/Cr⁴⁺:YAG self-Raman laser. In Fig. 5, spectra of the self-Raman laser output are recorded for a pumping power of 2 W, for Cr^{4+}:YAG crystal with an initial transmittance of 92% and the output mirror S1. As shown in Fig. 5, the spectral line at 1067 nm corresponds to the fundamental laser, while that at 1181 nm represents the first Stokes laser generated through the SRS process based on the main Raman mode at 901 cm^{-1}. The presence of only one Raman line in the spectra is attributed to the maximum Raman gain coefficient of the main Raman mode at 901 cm^{-1}.

A Cr^{4+}:YAG crystal with a transmittance of $T_0 = 92\%$ is initially employed to investigate passively *Q*-switched Nd: KGW/Cr⁴⁺:YAG self-Raman laser. Figure 6(a), (b) and (c)

Fig. 5 Spectra of self-Raman laser output for the pumping power of 2 W, for Cr⁴⁺:YAG crystal with initial transmittance of 92% and the output mirror S1
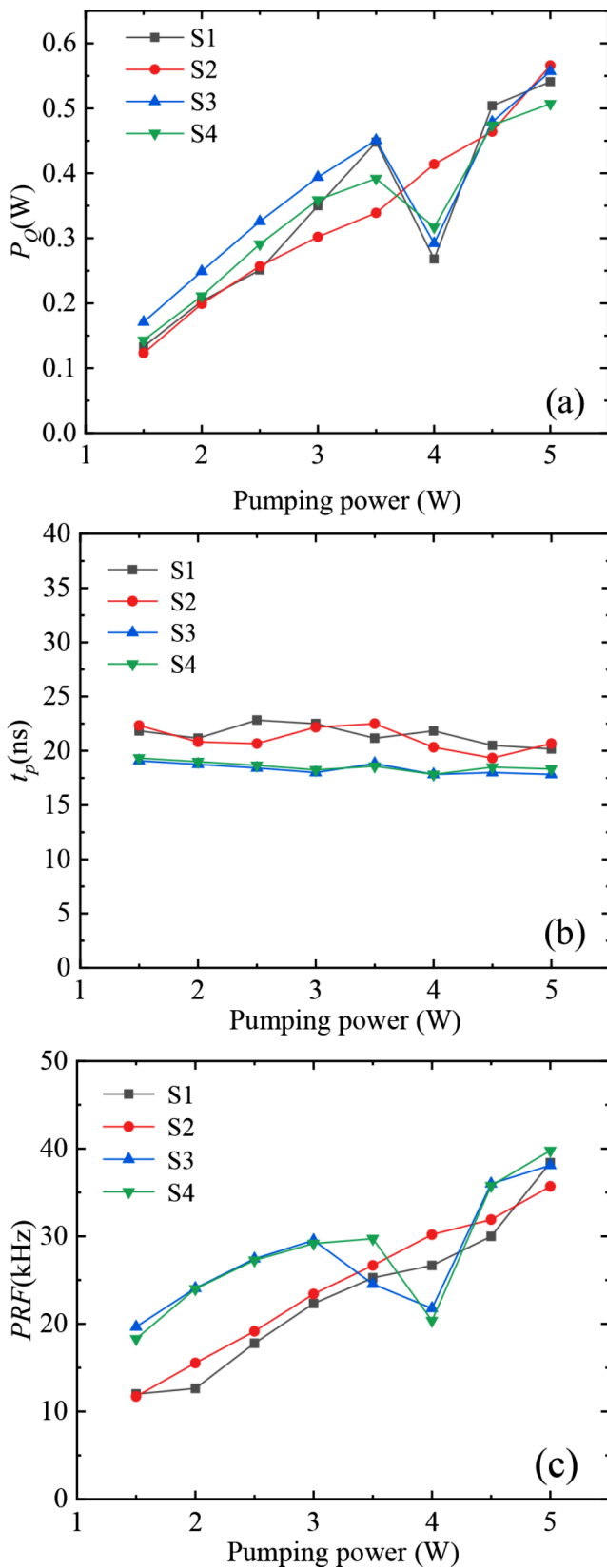
Fig. 6 Average output power (**a**), pulse width (**b**), and PRF (**c**) of the first Stokes laser is shown for Cr: YAG with an initial transmittance of $T_0 = 92\%$. The square, circle, triangle and inverted triangle symbols correspond to output mirrors S1, S2, S3 and S4, respectively

depict the average output power, pulse width and PRF of the first Stokes laser as the pumping power increasing, respectively. The square, circle, triangle and inverted triangle symbols correspond to output mirrors S1, S2, S3 and S4, respectively.

From Fig. 6(a), the output power of first Stokes laser increases with pumping power, and there is an extraordinary decrease for the pumping power of 4 W with S1, S2 and S3, which is attributed to thermal effects. In 2009, P. A. Loiko et al. conducted a comparative study on the thermal lensing effect in diode pumped N_g and N_p-cut Nd: KGW laser crystals, with output laser emission polarized along N_m [23]. For N_p-cut Nd: KGW, strong astigmatism was observed, with the refractive powers in the N_g- and N_m-directions exhibiting opposing signs. The study involved measuring the dependence of the thermal lensing dioptric power D as a function of pumping intensity $P_p/\pi\omega_p^2$ for the N_p-cut Nd: KGW crystals, where P_p is the pumping power, and ω_p is the radius of pumping beam. These dependencies were found to be linear with pumping intensity, allowing for the calculation of thermal lensing sensitivity factors $M = D/(P_p/\pi\omega_p^2)$, in units of dioptric power per (W/cm²): $(M_{Np-cut})_{Nm} = 0.85 \times 10^{-2}$ (N_p-cut Nd: KGW, N_m-direction), and $(M_{Np-cut})_{Ng} = -2.0 \times 10^{-2}$ (N_p-cut Nd: KGW, N_g-direction).

The observation of strong astigmatism and opposing signs of refractive powers in the N_g- and N_m-directions for N_p-cut Nd: KGW highlight the complex thermal effects influencing the operation of lasers based on Nd: KGW. Additionally, the thermal lensing of the Cr^{4+}:YAG crystal also impacts resonator stability [24, 25], leading to abnormal phenomena in laser output. Our research group intends to conduct a detailed investigation into the thermal effects on passively Q-switched Nd: KGW/Cr^{4+}:YAG self-Raman lasers.

With a pumping power of 5 W and S2 mirror, the maximum output power of first Stokes laser is 0.566 W, with an optical-to-optical efficiency of 11.3% and a pulse energy of 15.9 μJ. Figure 6(b) demonstrates that the pulse width of first Stokes laser is stable for all four output mirrors, with S3 and S4 having narrower pulse widths than S1 and S2. The narrowest pulse width, recorded with a pumping power of 5 W and S3 mirror, is 17.8 ns. Figure 6(c) indicates that PRF of the S1 and S2 mirrors increases with increasing pumping power. However, PRF of the S3 and S4 mirrors experiences a local decrease at a pumping power of 4 W. PRF of S3 and S4 mirrors surpasses that of S1 and S2 mirrors. At a pumping power of 5 W, the maximum PRF is 39.8 kHz.

In Fig. 7, for a Cr^{4+}:YAG crystal with an initial transmittance of $T_0 = 92\%$ and a pumping power of 2.5 W, pulse waveforms (a), (c), (e) and (g) and pulse sequences (b), (d), (f) and (h) of the first Stokes laser are recorded using S1, S2, S3 and S4, respectively. As shown in Fig. 7 (a), (c), (e)
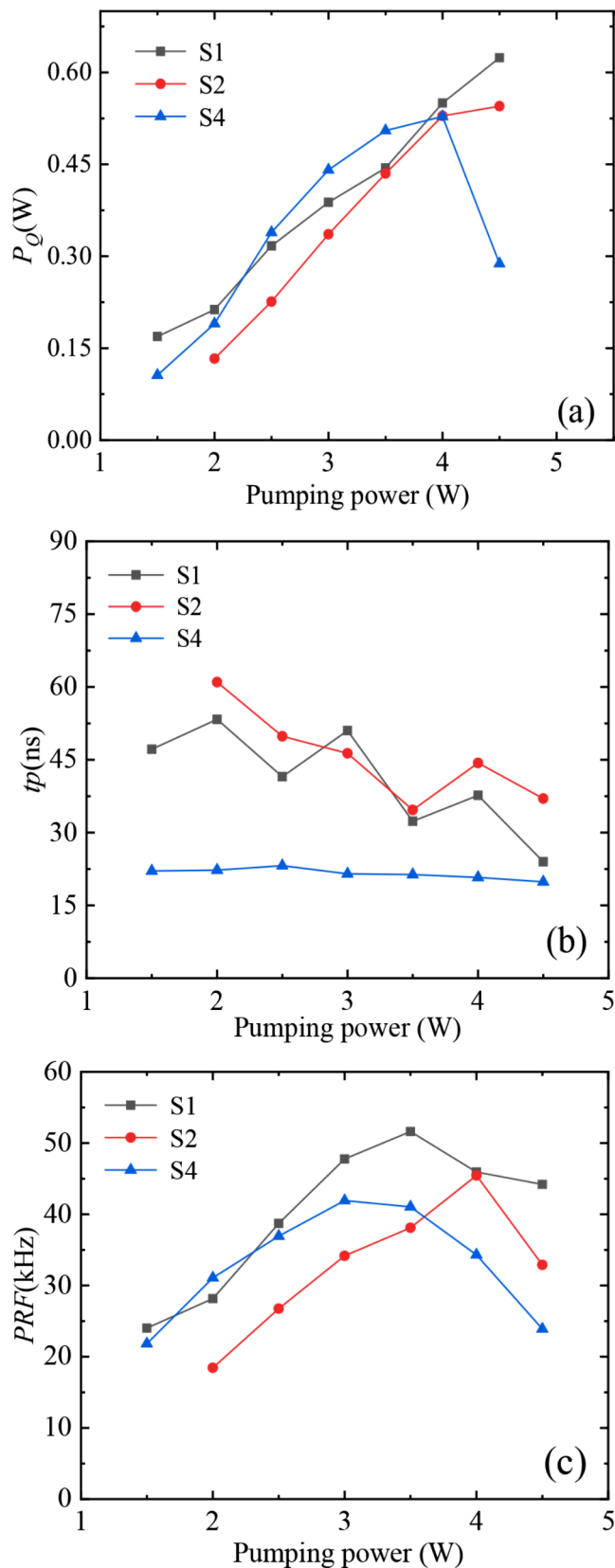
Fig. 7 For Cr^{4+}:YAG with an initial transmittance of $T_0 = 92\%$ and a pumping power of 2.5 W, pulse waveforms (**a**), (**c**), (**e**) and (**g**) and pulse sequences (**b**), (**d**), (**f**) and (**h**) of the first Stokes laser are recorded using S1, S2, S3 and S4, respectively
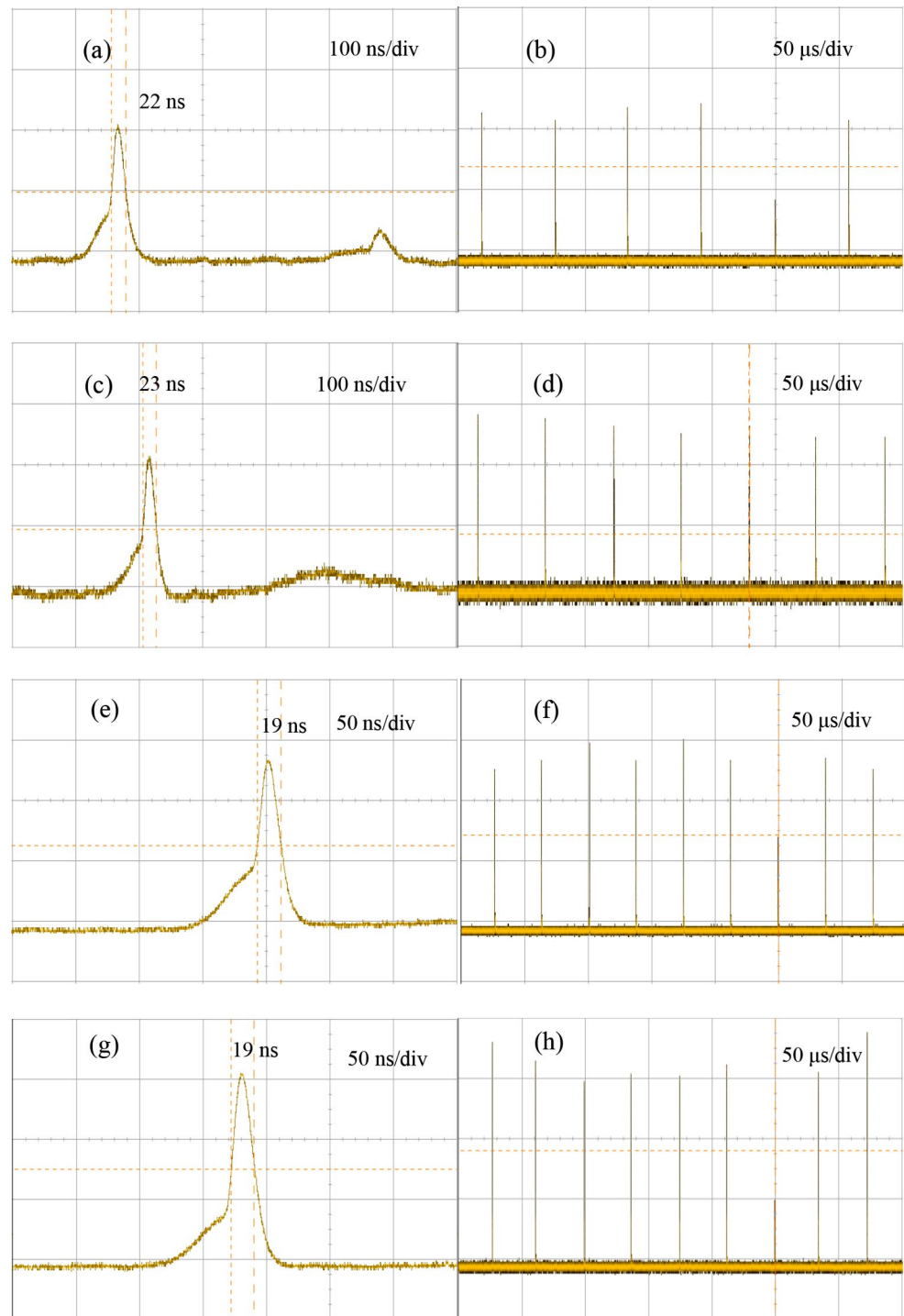
and (g), smaller reflectance of the output mirror leads to narrower pulse widths, and slight multi-pulse phenomena are observed with S1 and S2. As shown in Fig. 7 (b), (d), (f) and (h), pulse sequences of the first Stokes are stable.

Subsequently, experiments are conducted using a Cr^{4+}:YAG crystal with an initial transmittance of $T_0 = 96\%$ in the passively Q-switched Nd: KGW self-Raman laser. Stable operation of passively Q-switched Nd: KGW

self-Raman laser is not accomplished with S3. Figure 8(a), (b) and (c) illustrate the variations in the average output power, pulse width, and PRF of the first Stokes laser with the pumping power. The square, circle, and triangle symbols correspond to the output mirrors S1, S2 and S4, respectively. In Fig. 8(a), the output power of the first Stokes laser increases with the pumping power. However, for S2 and S4 mirrors, a sudden drop in output power occurs at pumping

Fig. 8 Average output power (**a**), pulse width (**b**), and PRF (**c**) of the first Stokes laser is shown for Cr: YAG with an initial transmittance $T_0 = 96\%$. The square, circle, and triangle symbols correspond to output mirrors S1, S2 and S4, respectively

powers of 4.5 W and 4 W, respectively, due to unstable cavity resonance caused by thermal lensing. When the pumping power is 4.5 W and the output mirror is S1, the maximum output power is 0.624 W, with an optical-to-optical efficiency of 13.9%, a pulse energy of 14.1 μJ, and a peak power of 0.588 MW. Figure 8(b) indicates good stability in the output pulse width, with S4 having a narrower pulse width than S2 and S1. When the pumping power is 4.5 W, the pulse width of the first Stokes laser is 19.8 ns with S4. Figure 8(c) shows that PRF of the first Stokes laser increases with the pumping power. When the pumping power is 3.5 W, and the output mirrors are S1 and S4, PRF rapidly decreases. Similarly, when the pumping power is 4 W, a rapid decrease in PRF is observed with the output mirror S2.

In Fig. 9, For a Cr^{4+}:YAG crystal with an initial transmittance of $T_0 = 96\%$ and a pumping power of 2.5 W, pulse waveforms (a), (c) and (e) and pulse sequences (b), (d) and (f) of the first Stokes laser are recorded using output mirrors S1, S2 and S4, respectively. As shown in Fig. 9 (a), (c) and (e), a smaller reflectance of the output mirror corresponds to a narrower pulse width of the first Stokes laser. Due to the high initial transmittance of Cr: YAG, there is no apparent occurrence of multiple-pulse phenomena. Figure 9 (a), (c) and (e) show the pulse sequences of the first Stokes laser, indicating stable pulse sequences.

5 Conclusion

In this paper, the end-pumped passively Q-switched Nd: KGW/Cr^{4+}:YAG self-Raman laser is designed to achieve high efficient operation. Concave-plane linear cavity is adopted to obtain the shortest cavity length, and long Nd: KGW crystal of 40 mm is used in the experiment. Cr^{4+}:YAG crystals of high initial transmittances ($T_0 = 96\%$ and 92%) are utilized to realize efficient and stable passively Q-switched operation. Stimulated Raman scattering is facilitated through the main Raman mode at 901 cm^{-1}, resulting in the generation of the first Stokes laser at 1181 nm. Notably, the laser achieves an optical-to-optical conversion efficiency of 13.9%, with a maximum output power of 0.624 W.

Fig. 9 For a Cr^{4+}:YAG crystal with an initial transmittance of $T_0 = 96\%$ and a pumping power of 2.5 W, pulse waveforms (**a**), (**c**), and (**e**) and pulse sequences (**b**), (**d**), and (**f**) of the first Stokes laser are recorded using output mirrors S1, S2 and S4, respectively
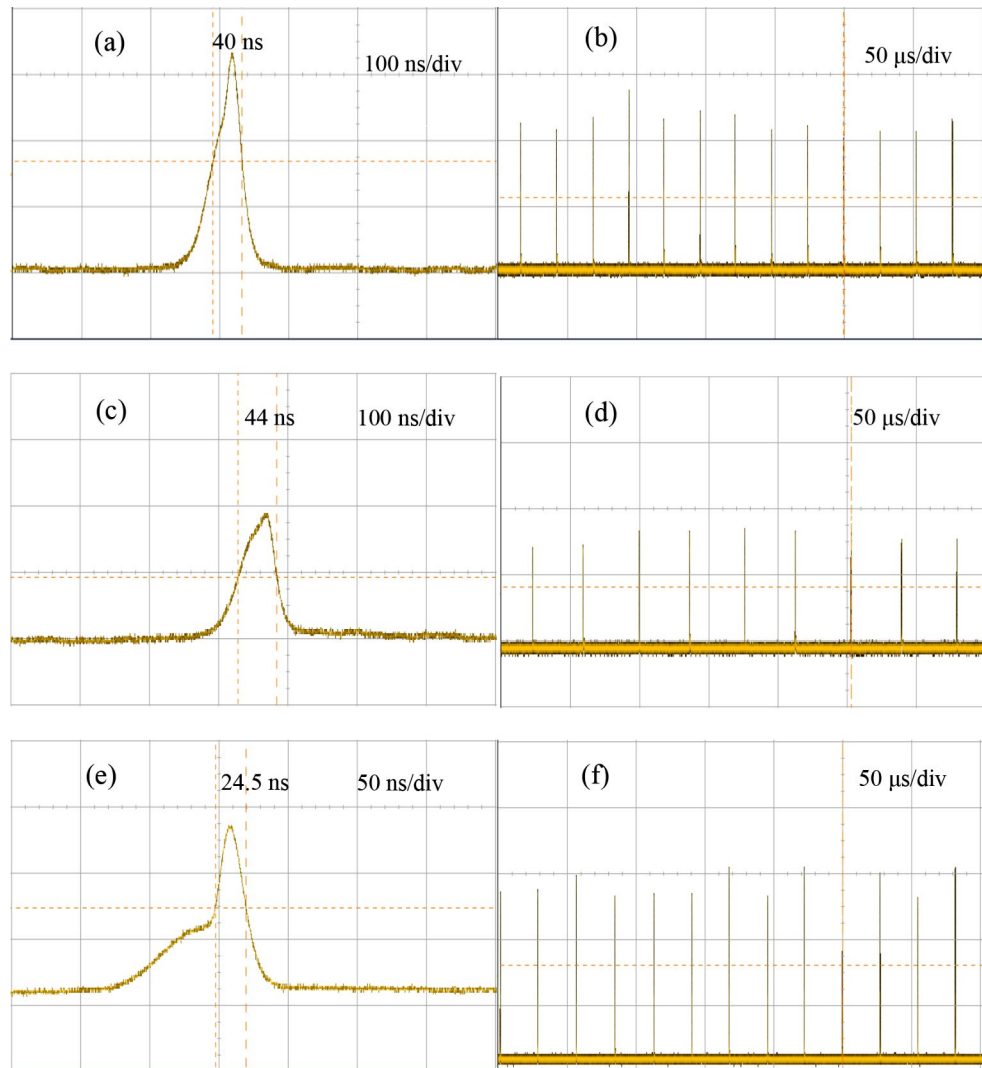
Author contributions Zou Qiaoshuang: Data curation, Writing-Original draft preparation.Sun Qinghu: Formal analysis, Visualization.Dai Zhenhong: Reviewing &editing.Ding Shuanghong: Conceptualization, Investigation, Methodology.

Data availability No datasets were generated or analysed during the current study.

Declarations

Competing interests The authors declare no competing interests.

References

1. O. Musset, Comparative laser study of nd:KGW and Nd: YAG near 1.3 μm. Appl. Phys. **64**, 503–506 (1997)

2. R.P. Mildren, J.A. Piper, Increased wavelength options in the visible and ultraviolet for Raman lasers operating on dual Raman modes. Opt. Express. **16**, 3261–3272 (2008)

3. X.L. Lv, J. Chen, Y. Peng et al., Investigation of high-energy extracavity Raman laser oscillator and single-pass Raman generator based on potassium gadolinium tungstate (KGW) crystal, opt. Laser Technol. **140**, 107023 (2021)

4. C. Yang, H.P. Peng, M. Chen et al., 1 kHz dual sub-pulse train picosecond radially polarized beam KGW raman generator capable of achieving multiple optical communication wavelength. Opt. Commun. **452**, 481–486 (2019)

5. H.M. Pask, Continuous-wave, all-solid-state, intracavity Raman laser. Opt. Lett. **30**, 2454–2456 (2005)

6. M.S. Ferreira, H.M. Pask, N.U. Wetter et al., Nd: YLF/KGW intracavity Raman laser in DBMC configuration at 1147 and 1163 nm in TEM₀₀. Solid State Lasers XXIX: Technol. Devices **11259** (2020)

7. M.S. Ferreira, H.M. Pask, N.U. Wetter, Intracavity diode-side-pumped Raman laser at 1147 nm and 1163 nm, Laser. Resonators, Microresonators, and Beam Control XX. SPIE 10518, 161–169 (2018)

8. Y.F. Chen, C.M. Chen, C.C. Lee et al., Efficient solid-state Raman yellow laser at 579.5 nm. Opt. Lett. **45**, 5612–5615 (2020)

9. J.G. Geng, Q. Sheng, S. Fu et al., Efficient continuous-wave nd:YVO$_4$/KGW intracavity Raman laser. Opt. Lett. **48**, 6364–6367 (2023)

10. H.J. Huang, Y.H. Fang, C.L. Chen et al., Compact continuous-wave solid-state Raman lasers at 707 and 714 nm for laser trapping and cooling of atomic strontium and radium. Opt. Lett. **48**, 4645–4648 (2023)

11. Y. Sun, C. Lee, Z. Zhu et al., Dual-polarization balanced yb:GAB crystal for an intracavity simultaneous orthogonally polarized multi-wavelength KGW Raman laser. Opt. Express. **6**, 3550–3557 (2016)

12. S.B. Dai, H. Zhao, Z.H. Tu et al., High-peak-power narrowband eye-safe intracavity Raman laser. Opt. Express. **28**, 36046–36054 (2020)

13. H. Zhao, C.H. Lin, C. Jiang et al., Wavelength-versatile deep-red laser source by intracavity frequency converted Raman laser. Opt. Express. **31**, 265–273 (2023)

14. H. Zhao, C.H. Lin, J.Y. He et al., Nanosecond pulsed deep-red Raman laser based on the nd:YLF dual-crystal configuration. Opt. Lett. **49**, 1009–1012 (2024)

15. H.W. Yang, J.X. Zhao, H.T. Huang et al., The first-stokes pulse generation in nd:KGW intracavity driven by a diode-pumped passively Q-switched nd: YAG/Cr^{4+}: YAG laser. Laser Phys. **21**, 343–347 (2011)

16. J.C. Chen, Y.W. Ho, Y.C. Tu et al., High-peak-power passively Q-switched laser at 589 nm with intracavity stimulated Raman scattering. Cryst. **13**, 334 (2023)

17. J.C. Chen, Y.C. Tu, Y.W. Ho et al., Highly efficient diode-pumped passively Q-switched nd:YVO$_4$/KGW raman lasers at yellow and orange wavelengths. Opt. Express. **31**, 8696–8703 (2023)

18. A.S. Grabtchikov, A.N. Kuzmin, V.A. Lisinetskii et al., All solid-state diode-pumped Raman laser with self-frequency conversion. Appl. Phys. Lett. **75**, 3742–3744 (1999)

19. V.A. Lisinetskii, A.S. Grabtchikov, A.A. Demidovich et al., Nd:KGW/KGW crystal: efficient medium for continuous-wave intracavity Raman generation. Appl. Phys. B **88**, 499–501 (2007)

20. A.J. Lee, H.M. Pask, D.J. Spence et al., *Generation of Yellow, continuous-wave Emission from an Intracavity, frequency-doubled Nd:KGW self-Raman Laser, Advanced Solid-State Photonics* (Optica Publishing Group, 2010), p. ATuA22

21. K. Huang, W.Q. Ge, T.Z. Zhao et al., High-power passively Q-switched nd:KGW laser pumped at 877 nm. Appl. Phys. B **122**, 1–7 (2016)

22. S. Ding, X. Zhang, Q. Wang, J. Zhang et al., Numerically modeling of passively Q-switched intracavity Raman lasers. J. Phys. D: Appl. Phys. **40**, 2736–2747 (2007)

23. P.A. Loiko, K.V. Yumashev, N.V. Kuleshov et al., Thermal lens study in diode pumped *Ng*- and *Np*-cut nd:KGd(WO$_4$)$_2$ laser crystals. Opt. Express. **17**, 23536–23543 (2009)

24. J. Song, C. Li, K.I. Ueda et al., Thermal influence of saturable absorber in passively Q-switched diode-pumped cw nd:YAG/Cr^{4+}:YAG laser. Opt. Commun. **177**, 307–316 (2000)

25. A.V. Kir'yanov, Y.O. Barmenkov, M.D. Rayo et al., Ground-state absorption saturation and thermo-lensing effect as main sources of refractive index non-linear change in Cr^{4+}:YAG at CW 1.06 μm excitation. Opt. Commun. **213**, 151–162 (2002)